Electronic Supplementary Material (ESI) for Journal of Materials Chemistry C.

Electronic Supplementary Information

Composition-tunable 2D $SnSe_{2(1-x)}S_{2x}$ alloys towards efficient bandgap engineering and high performance (opto)electronics

Yan Wang,[a] Le Huang, [a] Bo Li, [a] Jimin Shang,[a] Congxin Xia,[b] Chao Fan,[c] Hui-Xiong Deng,[a] Zhongming Wei,[a,*] and Jingbo Li[a,*]

[a.] *State Key Laboratory for Superlattices and Microstructures, Institute of Semiconductors, Chinese Academy of Sciences, Beijing 100083, China. *E-mail: zmwei@semi.ac.cn, jbli@semi.ac.cn*

[b.] *Department of Physics, Henan Normal University, Xinxiang 453007, China.*

[c.] *School of Electronics and Information Engineering, Hebei University of Technology, Tianjin 300401, China.*

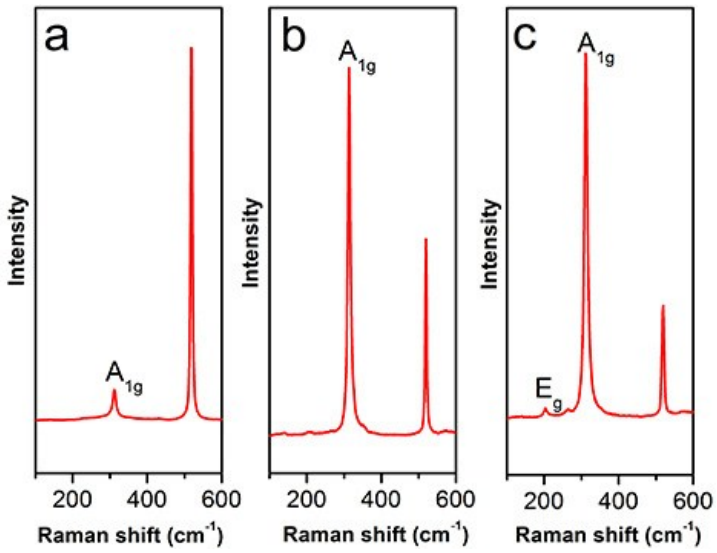

Figure S1. Raman spectra of layered SnS2 with various thickness. With the thickness of the samples decreasing, the Eg mode at 210 cm-1 become undetectable.

As shown in **Figure S1**, the peak at 514 cm^{-1} is a 300nm SiO_2 Raman peak of SiO_2/Si substrate, and the comparison of this SiO_2 Raman peak with 313 cm^{-1} can qualitatively shows the thickness of SnS_2 samples. With the thickness of the sample decreasing, the E_g mode at 210 cm^{-1} become undetectable. This can be attributed by the reduction of scattering centers for E_g mode with the thickness decrement of SnS_2 sample, which is in accordance with the previous reports[1-3].

Table S1 Compositions and lattice parameter c of $SnSe_{2(1-x)}S_{2x}$ alloys

x value in $SnSe_{2(1-x)}S_{2x}$ predecessor	Atomic % from XPS				XRD	
	Sn3d	Se3d	S	x' =S2p /(Se3d+ S2p)	2θ of (001) peak	c-axis $d_{spacing}$ (Å)
1	8.66	18.45	0	1	15.11	5.86
0.75	18.14	10.85	27.99	0.72	14.91	5.94
0.5	14.67	13.59	15.9	0.54	14.64	6.04
0.25	10.32	15.28	4.74	0.24	14.56	6.08
0	20.73	0	42.76	0	14.54	6.09

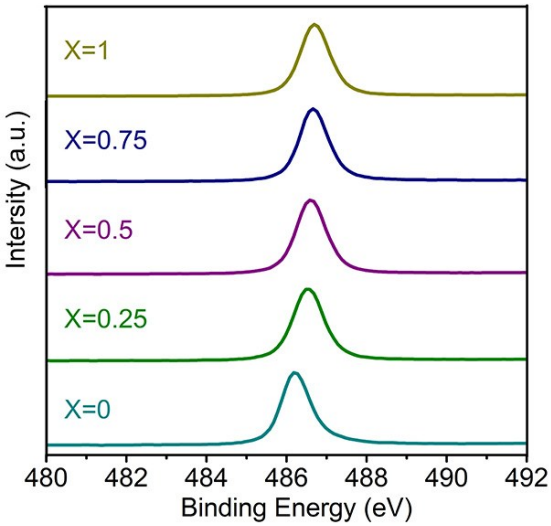

Figure S2 Sn 3d XPS spectra of bulk SnSe2(1-x)S2x samples.

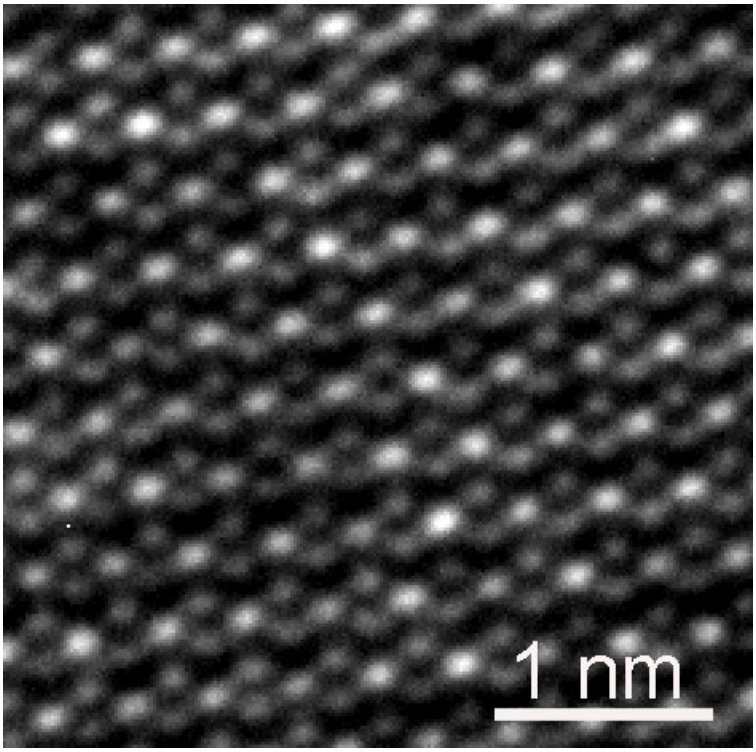

Figure S3. Naked HRTEM image of figure 3c which clearly shows three different level of brightness that presents different atoms for Sn, Se, and S in the alloy.

Computational methods

All the first-principles calculations in this work are performed by using the projector augmented wave (PAW)[4, 5] formalism within the frame work of density functional theory (DFT) in the Vienna ab initio Simulation Package (VASP)[6]. The generalized gradient approximation (GGA) of Perdew, Burke and Ernzerhof (PBE) functional[7] is adopted for electron exchange and correlation. A vacuum layer of no less than 15 Å is used to eliminate the interaction between adjacent images. The cutoff energy for the plane-wave basis set is set to 450 eV. A ($15 \times 15 \times 1$) Monkhorst-Pack *k*-point grid[8] is used to sample the first Brillouin zone of SnS_2 and $SnSe_2$ unitcells. Supercells consisting of 4×4 unit cells is constructed to simulate $SnS_{2x}Se_{2(1-x)}$ alloys with different concentrations.

The Brillouin zones of all the $SnS_{2x}Se_{2(1-x)}$ supercells are sampled with a $(5 \times 5 \times 1)$ for relaxations. All the structures are fully relaxed with a force tolerance of 0.02 eV/Å.

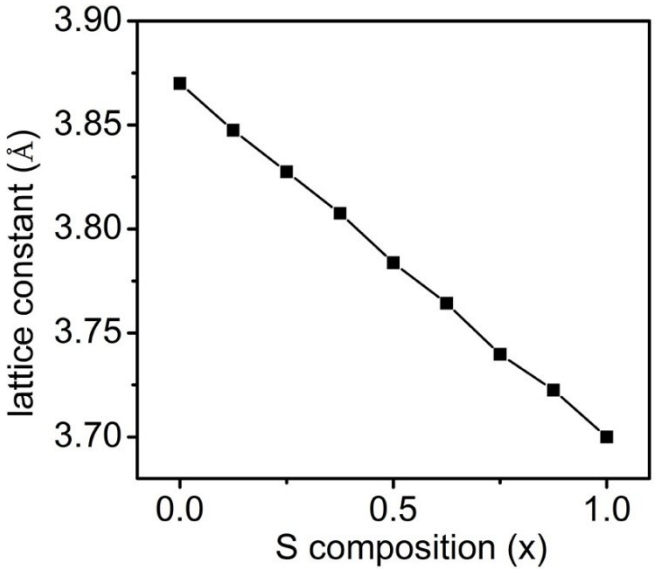

Figure S4. The lattice constant of $SnSe_{2(1-x)}S_{2x}$ alloy with S concentration that obtained from theoretical model.

As seen in **Figure S4**, the lattice constant value of SnSeS (x=0.5) model is about 0.378nm, which matches very well with the value measured from HRTEM image.

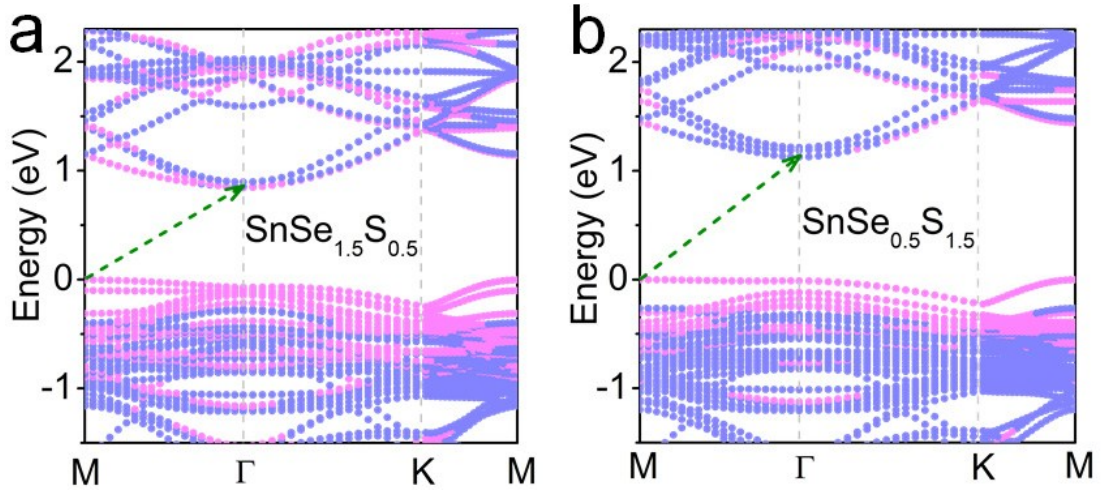

Figure S5. Calculated projected band structure of the different $SnSe_{2(1-x)}S_{2x}$ (a) x= 0.25 and (b) x=0.75 alloys. The blue and pink dots in the Figures denote the bands dominated by SnS_2 and $SnSe_2$, respectively.

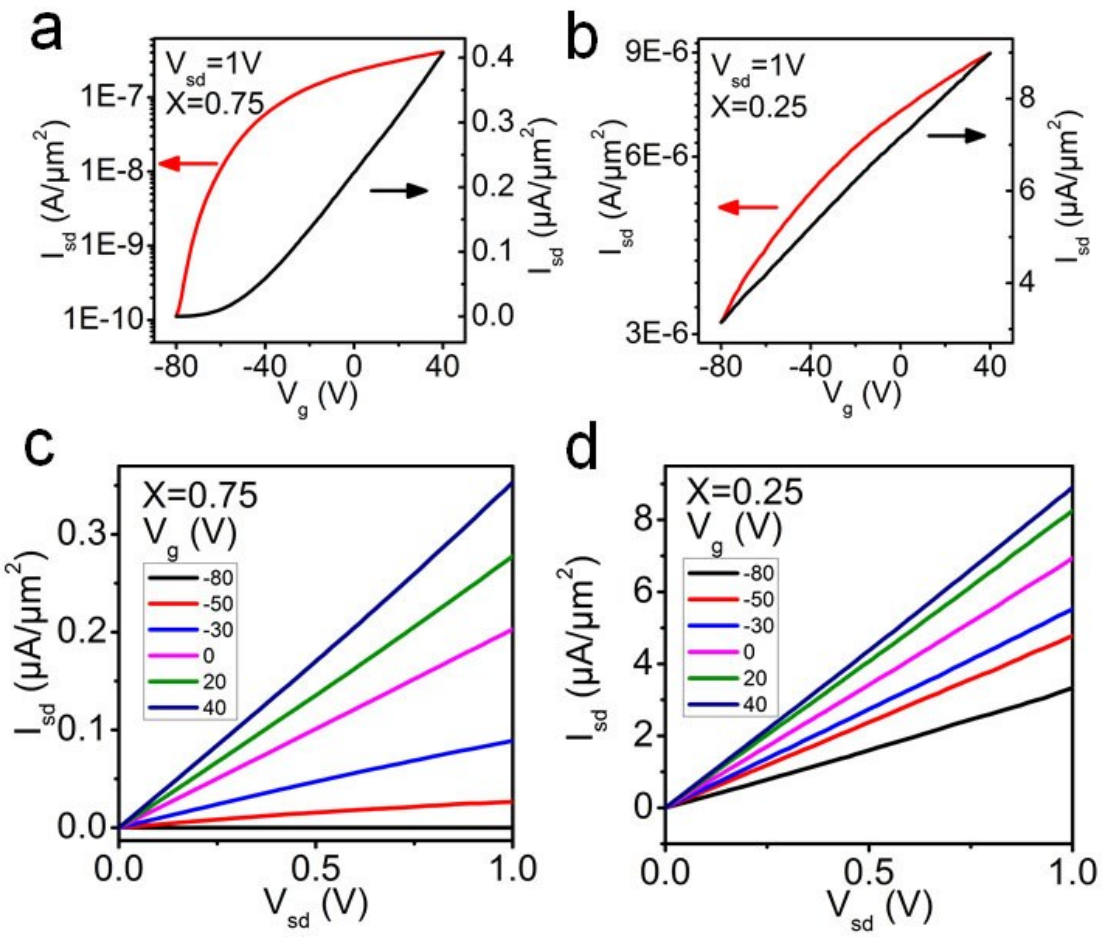

Figure S6. Transfer curves (I_{sd} - V_g) and output curves (I_{sd} - V_{sd}) of $SnSe_{2(1-x)}S_{2x}$ FETs for (a, c) x=0.75 and (b, d) x=0.25.

$SnSe_{2(1-x)}S_{2x}$ FETs with x=0.25 and 0.75 are fabricated, the output and transfer curves of which are shown in **Figure S4**. The field-effect mobility and 'ON/OFF' ratio of them are all calculated and shown in **Table 2**.

References:

1. X. Zhou, Q. Zhang, L. Gan, H. Q. Li and T. Y. Zhai, *Adv. Funct. Mater.*, 2016, **26**, 4405-4413.
2. J. H. Ahn, M. J. Lee, H. Heo, J. H. Sung, K. Kim, H. Hwang and M. H. Jo, *Nano Lett.*, 2015, **15**, 3703-3708.
3. S. D. Lei, L. H. Ge, Z. Liu, S. Najmaei, G. Shi, G. You, J. Lou, R. Vajtai and P. M. Ajayan, *Nano Lett.*, 2013, **13**, 2777-2781.
4. G. Kresse and J. Furthmuller, *Phys. Rev. B*, 1996, **54**, 11169-11186.
5. P. E. Blochl, *Phys. Rev. B*, 1994, **50**, 17953-17979.
6. G. Kresse and D. Joubert, *Phys. Rev. B*, 1999, **59**, 1758-1775.
7. J. P. Perdew, K. Burke and M. Ernzerhof, *Phys. Rev. Lett.*, 1996, **77**, 3865-3868.
8. H. J. Monkhorst and J. D. Pack, *Phys. Rev. B*, 1976, **13**, 5188-5192.